Hybrid Six-step Operation for Matrix Converter in Flywheel Energy Storage System

Jun-ichi Itoh, Takumi Masuda, Tsuyoshi Nagano, and Hayato Higa
Nagaoka University of Technology, Niigata, Japan

***Abstract*--This paper presents a hybrid six-step operation, which utilizes both a pulse width modulation (PWM) and a conventional six-step operation of a matrix converter in order to reduce switching losses during the standby time of flywheel. In the hybrid six-step operation, a virtual AC-DC-AC conversion is applied in order to separate the control of the matrix converter into a current source rectifier (CSR) control and a voltage source inverter (VSI) control. In particular, CSR is operated in PWM and VSI is operated in the six-step operation mode. Consequently, the switching loss of VSI is reduced as compared with the PWM operation due to the conventional six-step operation mode. In addition, the input current total harmonic distortion (THD) is improved as compared with the conventional six-step operation because the CSR modulation is PWM. In the experimental result, the input current THD of the hybrid six-step operation is improved by 76.0 % compared to the conventional six-step operation. Moreover, the efficiency of hybrid six-step operation was 1.0 % lower than the conventional six-step operation. In the hybrid the six-step operation, the input current THD is improved by 76.0 % in exchange for the drops of efficiency by 1.0 %.**

***Index Terms*--Flywheel energy storage system (FESS), matrix converter, six-step operation, pulse width modulation (PWM).**

I. INTRODUCTION

Recently, renewable energy systems such as photo voltaic (PV) and wind turbine have attracted many attentions [1-17]. In these system, a power fluctuation occurs due to meteorological conditions. Therefore, renewable energy systems require energy storage devices such as batteries, electric double layer capacitors (EDLC) or flywheels. The battery can achieve a high energy density at low cost. However, one of the problems in the battery energy storage is the short life time. In particular, the lifetime of the battery depends on the ambience and the number of charge/discharge time. In addition, the battery cannot cope with rapid charge/discharge owing to a large internal resistance. Meanwhile, the solution with EDLC provides a rapid charge/discharge because the internal resistance is very small. Moreover, the charge/discharge efficiency of EDLC is higher than batteries. However, the EDLC lifetime is still affected by the ambient temperature. In addition, energy density is not high.

On the other hand, a flywheel has a long lifetime due to no chemical structure. Thus the charge/discharge characteristics achieve high performance in contrast to the chemical battery. In addition, the flywheels provide an environmental friendly and low maintenance cost. Besides, the kinetic energy which is stored in the flywheel is proportional to the square of the rotational speed. Therefore, a flywheel energy storage system (FESS) can achieve a power leveling with high response to large power ripple [12-17].

Meanwhile, a matrix converter has attracted a lot of attentions as an AC-AC converter with many desirable features. The matrix converter is expected to achieve higher efficiency, smaller size and longer life-time compared to Back-To-Back (BTB) system because an energy buffer such as a large electrolytic capacitor and the step-up reactor is unnecessary. Therefore, the power leveling system that combines the matrix converter and FESS has been researched actively [18].

During the standby time, the flywheel standby losses such as windage and bearing losses still occur. Consequently, although the power fluctuation compensation is not required, it is necessary for the matrix converter to supply the energy consumed by the standby losses. During this period, the matrix converter is operated at the light load, the switching loss in which is predominant. The switching loss of the matrix converter using PWM becomes large in the standby mode because the number of the switching times is proportional to the switching frequency. In order to reduce the switching loss, the conventional six-step operation for the matrix converter has been proposed [19]. In the six-step operation, the switching loss is reduced because the PWM is not used. However, the input current THD increases due to the 120 deg. conduction mode. Furthermore, the filter loss also increases due to the distortion of the input current.

In this paper, the hybrid six-step operation for the matrix converter is proposed to reduce the switching loss in stand-by mode of FESS. In the proposed method based on the virtual AC-DC-AC conversion [20], the control of the matrix converter is separated into a current source rectifier (CSR) control and a voltage source inverter (VSI) control, where the CSR modulation is PWM and the VSI modulation is six-step operation. The switching loss of the matrix converter applied with the conventional six-step operation is reduced in compared with the PWM operation because the switching frequency of the six-step operation is six times of the output frequency. Meanwhile, the input current THD is reduced by the PWM operation of CSR. Moreover, the filter loss is reduced because the input current THD is improved compared with the conventional six-step operation. This paper is organized follows; first, the modulation of matrix converter based on the virtual AC-DC-AC conversion is introduced. Second, the hybrid

six-step operation is explained. Third, the validity of the hybrid six-step operation is confirmed by the simulation results and the experimental results. Finally, the converter loss of the hybrid six-step operation and the conventional six-step operation is compared

II. Circuit Configuration

A. Circuit Configuration

Fig. 1 shows a circuit diagram of the flywheel energy storage system using the matrix converter. The flywheel energy storage system compensates the power ripple caused by the renewable energy systems in order to smooth the grid power. In the standby mode of FESS, the converter is operated at the light load, the switching loss in which is predominant. However, PWM which can regulate the input current as a sine wave introduces the high switching loss. Therefore, the driving operation of a low switching loss is necessary in terms of a high efficiency. In addition, it is necessary to reduce the input filter loss which is increased by the input current distortion.

III. Modulation Strategy

A. Virtual AC-DC-AC Conversion

In this paper, the control method of matrix converter is based on the virtual AC-DC-AC conversion system, where the matrix converter is separated into a current source rectifier (CSR) and a voltage source inverter (VSI) as an indirect matrix converter [20].

Fig. 2 shows a circuit diagram of the matrix converter. The matrix converter of Fig. 2 is applied as the AC-AC converter in the flywheel energy storage system. Equation (1) expresses the relationship between the input voltage $^t[v_r\ v_s\ v_t]$ and the output voltage $^t[v_u\ v_v\ v_w]$ in the matrix converter of Fig. 2.

$$\begin{bmatrix} v_u \\ v_v \\ v_w \end{bmatrix} = \begin{bmatrix} s_{ru} & s_{su} & s_{tu} \\ s_{rv} & s_{sv} & s_{tv} \\ s_{rw} & s_{sw} & s_{tw} \end{bmatrix} \begin{bmatrix} v_r \\ v_s \\ v_t \end{bmatrix} \quad (1)$$

where, s_{mn} is a switching function of the switch S_{mn}. s_{mn} is 1 when S_{mn} is turned on and s_{mn} is 0 when S_{mn} is turned off.

Fig. 3 shows a circuit diagram of the indirect matrix converter which is used to consider the hybrid six-step operation. The virtual AC-DC-AC conversion replaces the matrix converter illustrated in Fig. 2 by the combination of CSR and VSI as shown in Fig. 3 in order to obtain the designated switching pulse commands. In the indirect matrix converter as shown in Fig. 3, the relationship between the input voltage $^t[v_r\ v_s\ v_t]$ and the output voltage $^t[v_u\ v_v\ v_w]$ is represented by (2).

$$\begin{bmatrix} v_u \\ v_v \\ v_w \end{bmatrix} = \begin{bmatrix} s_{up} & s_{un} \\ s_{vp} & s_{vn} \\ s_{wp} & s_{wn} \end{bmatrix} \begin{bmatrix} s_{rp} & s_{sp} & s_{tp} \\ s_{rn} & s_{sn} & s_{tn} \end{bmatrix} \begin{bmatrix} v_r \\ v_s \\ v_t \end{bmatrix} \quad (2)$$

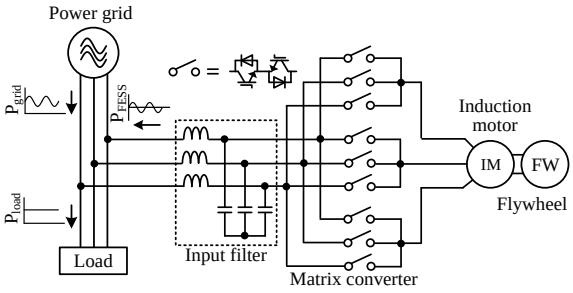

Fig. 1. Flywheel energy storage system using a matrix converter. FESS consists of the matrix converter, the flywheel and the input filter.

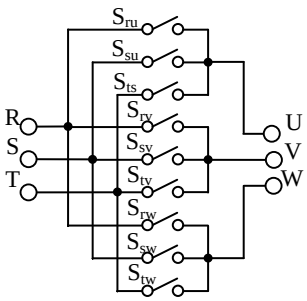

Fig. 2. Circuit diagram of matrix converter.

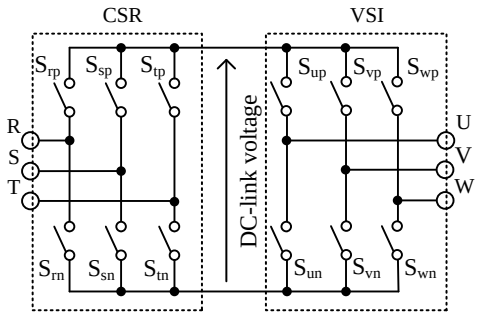

Fig. 3. Circuit diagram of an indirect matrix converter. Matrix converter separates the current source rectifier and the voltage source inverter using virtual AC-DC-AC conversion system.

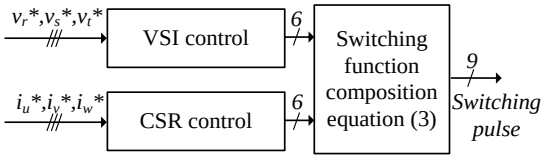

Fig. 4. Switching pulse generator. The switching pulses are generated by a virtual converter and a virtual inverter controls.

The relationship between the output voltage and the input voltage is determined solely by (2). In order to match the input and the output terminals of the indirect matrix converter and the matrix converter excluding the filter effect in Fig. 1, (3) should be satisfied.

$$\begin{bmatrix} s_{ru} & s_{su} & s_{tu} \\ s_{rv} & s_{sv} & s_{tv} \\ s_{rw} & s_{sw} & s_{tw} \end{bmatrix} = \begin{bmatrix} s_{up} & s_{un} \\ s_{vp} & s_{vn} \\ s_{wp} & s_{wn} \end{bmatrix} \begin{bmatrix} s_{rp} & s_{sp} & s_{tp} \\ s_{rn} & s_{sn} & s_{tn} \end{bmatrix} \quad (3)$$

Fig. 4 shows a switching pulse generator based on the virtual AC-DC-AC conversion. The method of the switching pulse generator is represented by (3). Thus, this method clearly separates the input current control and the

output voltage control.

B. PWM Operation

Table I shows the characteristics of the PWM operation, the conventional six-step operation and the hybrid six-step operation. In Table I of the characteristics of the PWM operation, the DC-link voltage waveform of PWM operation includes the switching frequency component. In addition, the input current of the PWM operation is controlled as a sine wave. However, the switching loss of the PWM operation is large because the number of switching times is proportional to the switching frequency. Meanwhile, the output voltage waveform of the PWM operation also introduces the high switching loss. In the standby time, the switching loss is predominant because the matrix converter is operated at the light load. Therefore, it is necessary to use the alternative modulation instead of PWM in order to reduce the switching loss.

C. Conventional Six-step Operation

In Table I of the characteristics of CSR as the conventional six-step operation, the DC-link voltage waveform of the conventional six-step operation includes the frequency component of the sixth order harmonics component. In addition, the conventional six-step operation is possible to greatly reduce the switching loss because the switching timing of the conventional six-step operation occurs every 120 deg. conduction of the fundamental frequency. Thus, the number of switching times is three times of fundamental frequency in the switching period. In VSI side with the conventional six-step operation, the output voltage waveform of the six-step operation includes the sixth order harmonics component. Thus, the conventional six-step operation is also possible to greatly reduce the switching loss because the switching timing of the conventional six-step operation is every 180 deg. conduction of the fundamental frequency. Thus, the number of switching times occurs at the second order harmonics component. However, the input filter loss is increased with the six-step operation. The input current is distorted because the input current of the conventional six-step operation is not controlled as the sine wave.

D. Hybrid Six-step Operation

In Table I of the characteristics of the hybrid six-step operation, the CSR modulation is PWM and the VSI modulation is 180 deg. conduction mode. Therefore, DC-link voltage includes the switching frequency component. The switching loss is reduced as compared with the full PWM operation. In addition, the input current total harmonics distortion is improved as compared with the conventional six-step operation because CSR modulation is PWM. Thus, the input filter loss is reduced compared with the conventional six-step operation.

Fig. 5 shows the modulation block diagram of the indirect matrix converter. In Fig. 5, CSR side is controlled by the input current commands. The input current command VSI side is controlled by output valtage

TABLE I
CHARACTERISTICS OF PWM, CONVENTIONAL SIX-STEP OPERATION AND HYBRID SIX-STEP OPERATION

	PWM operation	Six-step operation	Hybrid six-step operation
Input current	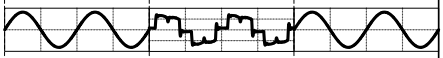		
CSR	PWM conduction	120 deg. conduction	PWM conduction
DC-link voltage	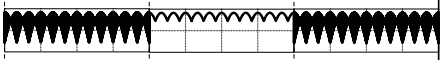		
VSI	PWM conduction	180 deg. conduction	180 deg. conduction
Output voltage	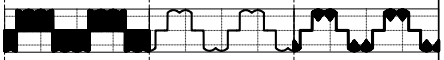		
Switching loss	Large	Low	Nearly low
Input filter loss	Low	Large	Nearly low

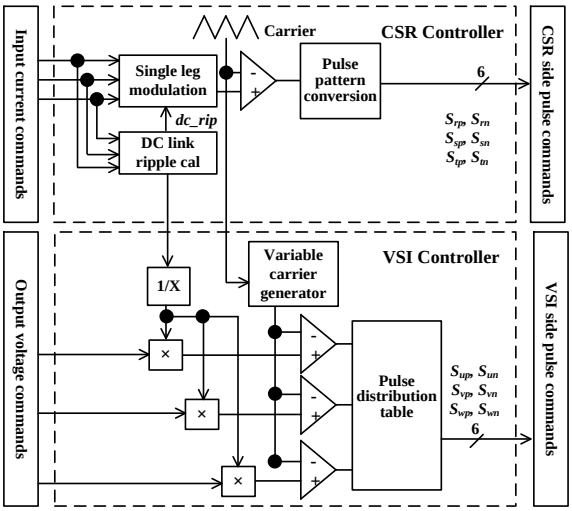

Fig. 5. Modulation block diagram of the indirect matrix converter.

commands.In Fig. 5, the matrix converter is used V / f control of VSI modulation.

IV. SIMULATION RESULTS

Fig. 6 and Table II show the simulation conditions to verify the fundamental operation of the hybrid six-step operation. This chapter presents the simulation results using a circuit diagram in Fig. 6 to confirm the reduction of the input current total harmonic distortion (THD) with the proposed hybrid six-step operation.

Fig. 7 shows the operation waveforms of the matrix converter in the full PWM operation. The output voltage is a sine wave in the PWM operation as Fig. 7, the input current THD is 1.40 %. However, the swithching loss is large because the number of switching times is high.

Fig. 8 shows the operation waveforms of the matrix converter in the conventional six-step operation when FESS is standby. The output voltage is the square waveform. Thus, the switching loss is reduced compared with the PWM operation. However, the output voltage is

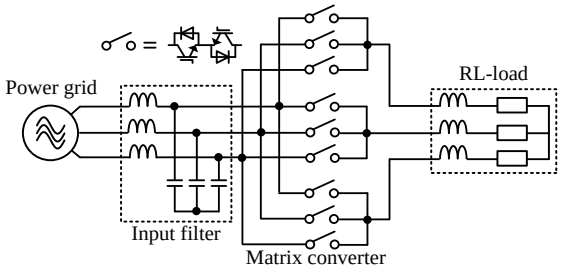

Fig. 6. Simulation circuit diagram of matrix converter connected RL-load.

TABLE II
SIMULATION PARAMETERS UNDER IDEAL CONDITION

Circuit parameter	Grid line voltage	200 V
	Input filter L	2 mH
	Input filter C	6.6 μF
	Carrier frequency	10 kHz
Load parameter	R-load	76 Ω
	L-load	10 mH

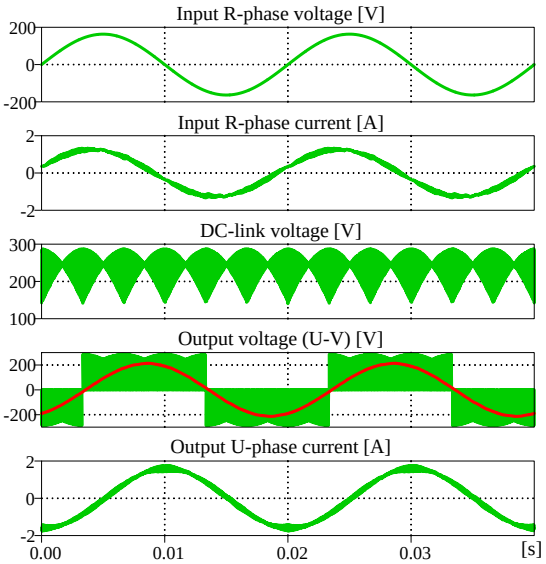

Fig. 7. Simulation results of PWM operation. The CSR operation is PWM. In the VSI, the PWM operation is used. The input current THD is 1.40%.

distorterd. In the output current of Fig. 8, the input current THD is 33.7 %. In addition, the filter loss is increased by the input current.

Fig. 9 shows the operation waveforms of the matrix converter in the hybrid six-step operation. The output voltage includes the 10 kHz component by PWM in the vicinity of the peak in the hybrid six-step operation. The output voltage waveform is a rectangular wave. In addition, the input current THD is 11.4 %. It is confirmed that the input current THD is reduced by 66.2 % than the conventional six-step operation.

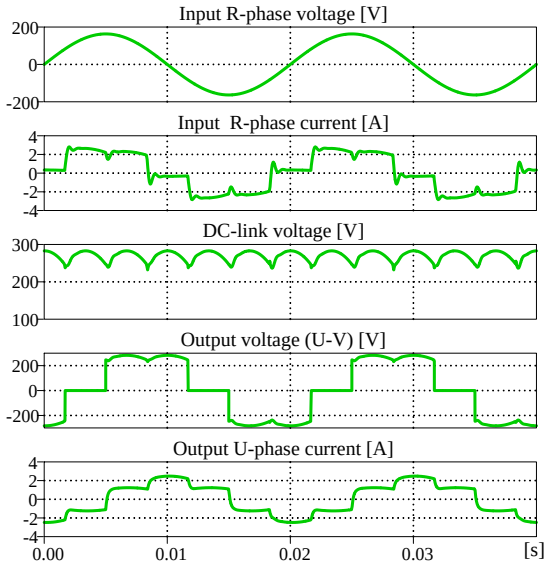

Fig. 8. Simulation results of six-step operation. The CSR operation is 120 deg. conduction. In the VSI, 180 deg. conduction is used. The input current THD is 33.7%. In the six-step operation, the switching loss is reduced compared to PWM operation.

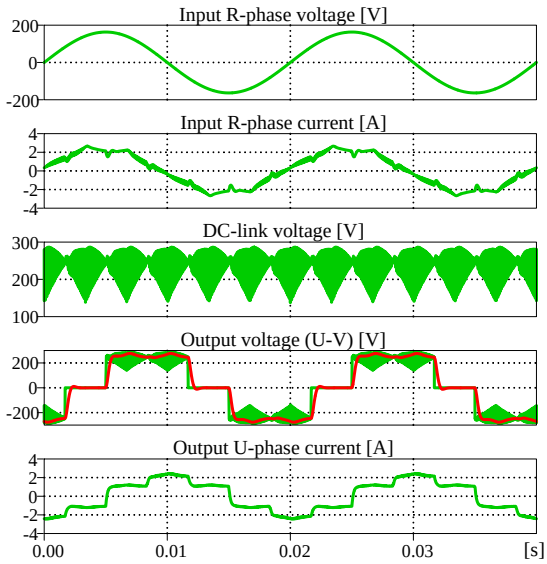

Fig. 9. Simulation results of hybrid six-step operation. The CSR operation is PWM operation. In the VSI, 180 deg. conduction is used. The input current THD is improved to 33 % compared with conventional six-step operation. In addition, the switching loss is also reduced compared to PWM operation.

V. EXPERIMENTAL RESULTS

A. PWM Operation

Fig. 10 and Table III show the experimental conditions. This chapter presents the experimental results using a prototype drawn in Fig. 10 to confirm the input current THD and the efficiency of the converter with the proposed the hybrid six-step operation.

Fig. 11 shows the experimental results when the matrix converter is applied with the full PWM operation. In Fig. 11, the output current is sinusoidal waveform by the PWM operation. However, the switching loss of the PWM operation is high

B. Conventional Six-step Operation

Fig. 12 shows the experimental results when the matrix converter is applied with the conventional six-step operation. In Fig. 12, the output voltage is the square waveform. Therefore, the switching loss is reduced because the switching times of the six-step operation are lower than the PWM operation. However, the input current THD is 36.7%. As a result, the input filter loss increases.

C. Hybrid Six-step Operation

Fig. 13 shows the experimental results when the matrix converter is applied with the hybrid six-step operation. In Fig. 13, the output voltage includes the switching ripple component at the peak of the output voltage. In the output voltage, it is nearly the square waveform, whereas the input current THD is 8.84 %. In the proposed hybrid six-step operation, the input current THD is reduce by 76.0 % as compared with the conventional six-step operation. It can be confirmed that the six times of the fundamental frequency is significantly reduced.

Fig. 14 shows the input current THD characteristic of PWM, conventional six-step operation and hybrid six-step operation. In the light load of Fig. 14, the input current THD of hybrid six-step operation is reduced to 25% compared to the conventional six-step operation. In addition, the input current THD of hybrid six-step operation is a lower than conventional six-step operation in a wide input power range.

D. Efficiency of Converter

Fig. 15 shows the efficiency characteristic of the conventional six-step operation and the hybrid six-step operation. In Fig. 15, the output power was varied from 200 W to 2.5 kW. In the conventional six-step operation, the efficiency is drops to 92.8 % in the heavy load because the input filter loss is increased by the distortion of the input current. In the light load, the efficiency of hybrid six-step operation is achieved to a more than 97.9 %. In conventional six-step operation, the maximum efficiency is achieved by 99.1 %. Thus, the hybrid six-step operation is a better efficiency than the conventional six-step operation in a low output power range. In addition, the hybrid six-step operation is the most efficient modulation method in a low output power range.

VI. Conclusions

This paper proposed the hybrid six-step operation, which utilizes both PWM and the conventional six-step operation, for reduction of the switching loss and the input current harmonics distortion. In the proposed method, the CSR modulation is PWM and the VSI modulation is 180 deg. conduction mode based on the virtual AC-DC-AC conversion. In the proposed hybrid six-step operation, the switching loss is reduced. In addition, the input current THD is improved as compared with the conventional six-step operation. From the experimental results, the input current THD was improved by 76.0 % as compared with the conventional six-step operation. In addition, the efficiency of the hybrid six-step operation was 1.0 % lower than the conventional six-step operation. In the hybrid the six-step operation, the input current THD was improved by 76.0 % in exchange for the drops of efficiency by 1.0 %.

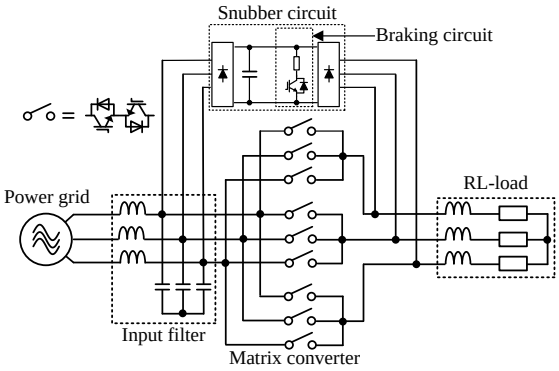

Fig. 10. Prototype of matrix converter connected RL-load.

TABLE III
Experimental Parameters of Prototype Condition

Circuit parameter	Grid line voltage	200 V
	Input filter L	2 mH
	Input filter C	6.6 μF
	Carrier frequency	10 kHz
Load parameter	R-load	25.3Ω
	L-load	5 mH

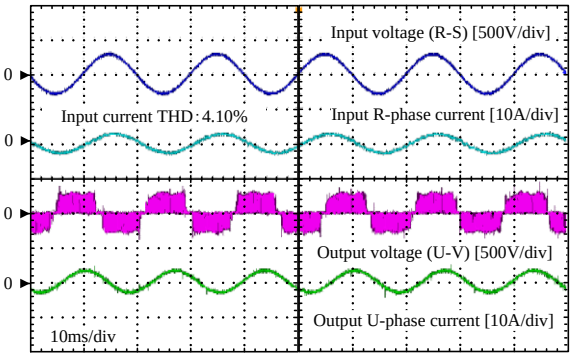

Fig. 11. Experimental results of PWM operation. The input current THD is 4.10 %.

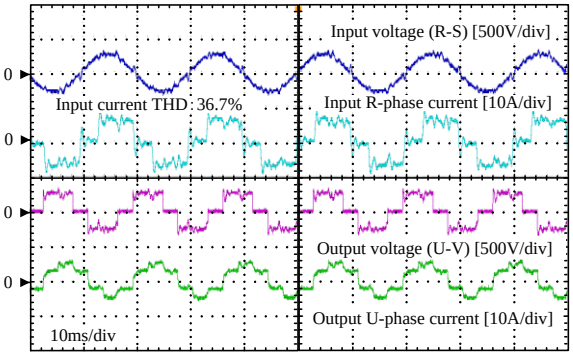

Fig. 12. Experimental results of conventional six-step operation. The switching loss is reduced by the conventional six-step operation. The input current THD is 36.7 %.

Acknowledgment

This work was supported by JSPS KAKENHI Grant Numbers JP15H03960.

REFERENCES

[1] F. Blaabjerg, et al., "Overview of Control and Grid Synchronization for Distributed Power Generation Systems", *IEEE Trans. Ind. Electron.*, vol. 53, no. 5, pp. 1398-1409 (2006).

[2] F. Blaabjerg, et al., "Power electronics as efficient interface in dispersed power generation systems", *IEEE Trans. Ind. Electron.*, vol. 19, no. 5, pp. 1184-1194 (2004).

[3] Josep M. Guerrero, et al., "Hierarchical Control of Droop-Controlled AC and DC Microgrids—A General Approach Toward Standardization", *IEEE Trans. Ind. Electron.*, vol. 58, no. 1, pp. 278-172 (2010).

[4] Nikolas Flourentzou, et al., "VSC-Based HVDC Power Transmission Systems: An Overview", *IEEE Trans. Power Electron.*, vol. 24, no. 3, pp. 592-602 (2009).

[5] J. P. Barton, et al., "Energy storage and its use with intermittent renewable energy", *IEEE Trans. Energy Conversion*, vol. 19, no. 2, pp. 441-448 (2004).

[6] Adnan Sattar, et al., "Real-Time Implementation of BESS to Smooth the Output Power Fluctuation of Variable Speed Wind Turbine Generator", *IEEJ Trans. Ind. Appl.*, vol. 3 no. 3 pp. 198-205 (2014).

[7] Takashi Suzuki, et al., "Introduction and Practical Use of Energy Storage System with Lithium-ion Battery for DC Traction Power Supply System", *IEEJ Trans. Ind. Appl.*, vol. 5, no. 1, pp. 20-25 (2016).

[8] Ritwik Chattopadhyay, et al., "Low-Voltage PV Power Integration into Medium Voltage Grid Using High-Voltage SiC Devices", *IEEJ Trans. Ind. Appl.*, vol. 4, no. 6, pp. 767-775 (2015).

[9] Hirokazu Seki, et al., "Deceleration Control System for Electric-Powered Wheelchairs with Efficient EDLC Charge/Discharge", *IEEJ Trans. Ind. Appl.*, Vol. 4, No. 1, pp. 11-19 (2015).

[10] Shota Yamaguchi, et al., "Single-phase Power Conditioner with a Buck-boost-type Power Decoupling Circuit", *IEEJ Trans. Ind. Appl.*, vol. 5, no. 3, pp. 191-198 (2016).

[11] J. M. Carrasco, et al., "Power-Electronic Systems for the Grid Integration of Renewable Energy Sources: A Survey", *IEEE Trans. Ind. Electron.*, vol. 53, no. 4, pp. 1002-1016 (2006).

[12] Srdjan M. Lukic, et al., "Energy Storage Systems for Automotive Applications", *IEEE Trans. Ind. Electron.*, vol. 55, no. 6, pp. 2258-2267 (2008).

[13] Sergio Vazquez, et al., "Energy Storage Systems for Transport and Grid Applications", *IEEE Trans. Ind. Electron.*, vol. 57, no. 12, pp. 3881-3895 (2010).

[14] H. Akagi, et al., "Control and performance of a doubly-fed induction machine intended for a flywheel energy storage system", *IEEE Trans. Ind. Electron.*, vol. 17, no. 1, pp. 109-116 (2002).

[15] Dong-Jing Lee, et al., "Small-Signal Stability Analysis of an Autonomous Hybrid Renewable Energy Power Generation/Energy Storage System Part I: Time-Domain Simulations", *IEEE Trans. Ind. Electron.*, vol. 23, no. 1, pp. 311-320 (2008).

[16] G. O. Cimuca, et al., "Control and Performance Evaluation of a Flywheel Energy-Storage System Associated to a Variable-Speed Wind Generator", *IEEE Trans. Ind. Electron.*, vol. 53, no. 4, pp. 1074-1085 (2006).

[17] Grzegorz Iwanski, et al., "DFIG-Based Power Generation System With UPS Function for Variable-Speed Applications", *IEEE Trans. Ind. Electron.*, vol. 55, no. 8, pp. 3047-3054 (2008).

[18] Bingsen Wang, et al., "Dynamic Voltage Restorer Utilizing a Matrix Converter and Flywheel Energy Storage", *IEEE Trans. Ind. Electron.*, vol. 45, no. 1, pp. 222-213 (2009).

[19] A. M. Khambadkone, " Compensated synchronous PI current controller in overmodulation range and six-step operation of space-vector-modulation-based vector-controlled drives ", *IEEE Trans. Ind. Electron.*, Vol. 49, No. 3, pp. 574-580 (2002)

[20] J. Itoh, I. Sato, H. Ohguchi, K. Sato, A. Odaka and N. Eguchi, "A Control Method for the Matrix Converter Based on Virtual AC/DC/AC Conversion Using Carrier Comparison Method", *IEEJ Trans.*, vol. 124-D, no. 5, pp. 457-463 (2004).

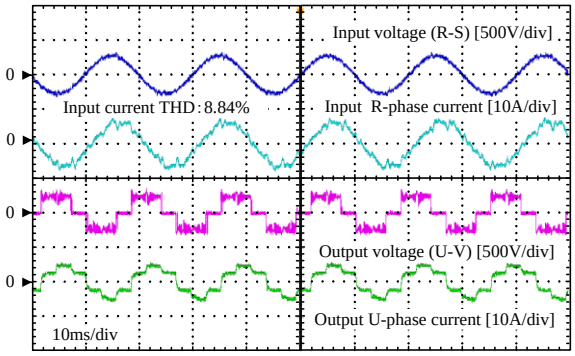

Fig. 13. Experimental results of hybrid six-step operation. The input current THD is improved by 76.0 % compared with the conventional six-step operation.

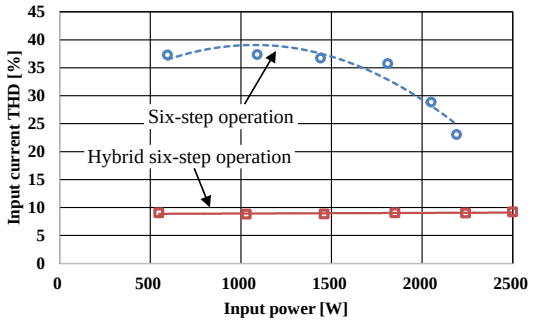

Fig. 14. Input current THD of conventional six-step operation and hybrid six-step operation. The input current THD of hybrid six-step operation is a lower than conventional six-step operation in a wide input power range.

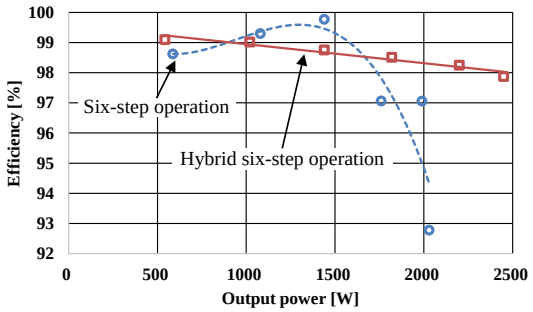

Fig. 15. Efficiency of conventional six-step operation and hybrid six-step operation. The efficiency is drops to 92.8 % in a high input power range. On the other hand, efficiency of hybrid six-step operation. The efficiency is achieved by more than 97.9 %. In addition, the maximum efficiency is achieved by 99.1 %.